

Full Classification of Transport on an Equilibrated 5/2 Edge via Shot Noise

Sourav Manna,^{1,2,*} Ankur Das,^{1,†} Moshe Goldstein,² and Yuval Gefen¹

¹*Department of Condensed Matter Physics, Weizmann Institute of Science, Rehovot 7610001, Israel*

²*Raymond and Beverly Sackler School of Physics and Astronomy, Tel-Aviv University, Tel Aviv 6997801, Israel*

The nature of the bulk topological order of the 5/2 non-Abelian fractional quantum Hall state and the steady-state of its edge are long-studied questions. The most promising non-Abelian model bulk states are the Pfaffian (Pf), anti-Pfaffian (APf), and particle-hole symmetric Pfaffian (PHPf). Here, we propose to employ a set of dc current-current correlations (*electrical shot noise*) in order to distinguish among the Pf, APf, and PHPf candidate states, as well as to determine their edge thermal equilibration regimes: full vs. partial. Using other tools, measurements of GaAs platforms have already indicated consistency with the PHPf state. Our protocol, realizable with available experimental tools, is based on fully electrical measurements.

Introduction.— Manifestations of non-Abelian braiding statistics [1] rely on foundational facets of strongly-correlated many-body platforms, and may pave the way towards establishing tools for topological quantum computation [2]. A potential host of such quasiparticles is the 5/2 fractional quantum Hall state [3, 4]. As far as the nature of the bulk state is concerned, there has been a number of proposals which lead to the same electrical Hall conductance but differ in their edge structure and the two-terminal thermal conductance. The three most prominent non-Abelian model states are the Pfaffian (Pf) [1], its hole-conjugate version — the anti-Pfaffian (APf) [5, 6], and the particle-hole symmetric Pfaffian (PHPf) [7–12]. Experimental measurements of two-terminal thermal conductance [13] can be explained invoking either the APf or the PHPf state. More recent experimental measurements of noise and thermal conductance are only consistent with the PHPf state [14, 15]. This is in contradiction with numerical evidence [16–24] supporting either the Pf or APf state. Other candidates include the Abelian 331, anti-331, 113 and K= 8 states [25–27] and non-Abelian SU(2)₂ and anti-SU(2)₂ states [28, 29], which are not consistent with experimental measurements [13–15].

Another important classification concerns the edge of such states. One may characterize the edge modes according to their degree of equilibration, which varies with the length of the edge. Previous studies [13, 15] have demonstrated that the degree of thermal equilibration, reached among the chiral modes, can be modified by changing the length of the edge/interface [14, 15]. Major differences in transport features may arise, depending on whether full or partial thermal equilibration is approached. Thus, characterization of thermal equilibration regimes is an outstanding problem. It has also been shown that the thermal equilibration length can be parametrically longer than the charge equilibration length [30–33]. It is then reasonable to assume full charge equilibration regardless the degree of thermal equilibration.

Measurements of shot noise and thermal conductance [14, 15] in a device made out of interfaces of the 5/2 state and Abelian integer states are only consistent with the

State \ Thermal equilibration	No equilibration	Partial equilibration	Full equilibration
Pf	✗ ✕ ✖ [Yutushui et al.]	✗ ✕ ✖	✗ ✕ ✖
APf	✗ ✕ ✖ [Yutushui et al.] [Park et al.]	✕ ✖ [Park et al.]	✗ ✕ ✖ [Park et al.]
PHPf	✗ [Yutushui et al.]		

TABLE I. Current experimental and theoretical status for classification of the non-Abelian 5/2 bulk states and their edge thermal equilibration regimes. Crosses (red, green, blue) represent the experimental exclusion of corresponding scenarios. Red, green, blue crosses exclude scenarios via measurements of two-terminal thermal conductance [13], interface noise [14], and interface thermal conductance [15], respectively. Theoretical proposals by Park et al. [34] and Yutushui et al. [35] used thermal transport with electrical shot noise at the edge and electrical transport with no equilibration, respectively, to confirm corresponding scenarios. Our work can distinguish among the yellow highlighted scenarios, thus completing the table.

PHPf state. A detailed theoretical model for the experiments in Ref. 14 and 15 was put forward in Ref. 36. Preceding to those experiments, a number of theoretical studies [34, 37–50] analyzed the Pf and APf states to explain the first thermal measurements on the 5/2 edge [13] along with some proposals [34, 35, 37, 38, 51] to distinguish the bulk state. In particular, Ref. 51 proposed that the Pf family members can be distinguished using their chiral gravitons, which does not rely on edge physics. Notably, Ref. 34 has addressed the challenges of identifying the underlying state taking into account different equilibration regimes. It was shown that electrical shot noise combined with thermal transport can uniquely point out the APf state, along with the degree of equilibration. Those works did not take into account that charge and thermal equilibration lengths can differ by order of magnitudes [30–33]. They also fall short (c.f. Table I) of providing unique diagnostics of the bulk topological state (Pf, APf, and PHPf) and, simultaneously, the thermal equilibration regime. This is the challenge addressed in this work.

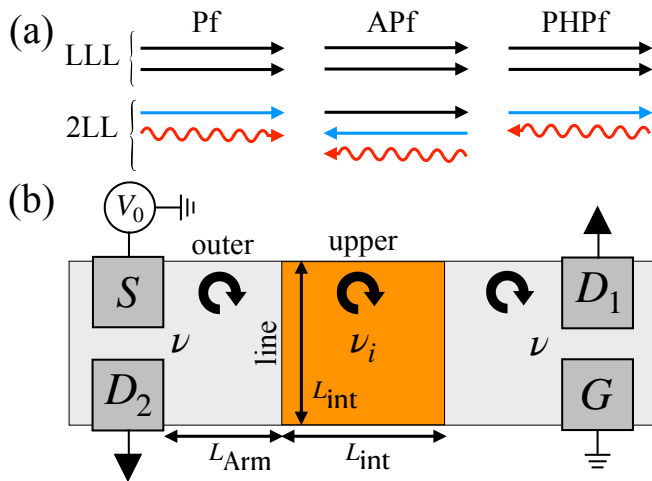


FIG. 1. (a) The edge structures of Pf, APf, and PHPf states: Integer, charge-1/2 boson [4], and charge-neutral Majorana modes are depicted as black, blue, and wiggly red lines, respectively. Arrowheads show the chirality. The lowest Landau level (LLL) is same for all three states but the second Landau level (2LL) is different. (b) Our proposed device: A middle region of the Hall bar is depleted from filling ν to filling $\nu_i (< \nu)$ creating two interfaces (“line”). Specifically, we take $\{\nu, \nu_i\}$ as $\{5/2, 2\}$ or $\{5/2, 7/3\}$ or $\{3, 5/2\}$. We call the boundary of the vacuum with ν the “outer”, and with ν_i the “upper”. We have four contacts, the source S (biased by a dc voltage V_0), a ground contact G , and two drains D_1, D_2 . Each circular arrow shows the chirality of charge propagation of the respective filling. The geometric lengths L_{Arm} and L_{int} are assumed to be of the same order of magnitude.

Our work relies on the setup depicted in Fig. 1, where current-current correlations (CCC) are computed when the 5/2 bulk state is interfaced with an Abelian quantum Hall state. We calculate both dc auto- and cross-correlations (from now on we drop the “dc” for simplicity). Our results can discriminate between the full and partial thermal equilibration regimes of the PHPf state. In addition, our protocol is unique in being able to distinguish among the Pf, APf, and PHPf states along with their thermal equilibration regimes: full vs. partial. Throughout the entire analysis, we assume that the charge equilibration length (full equilibration has been observed over a distance $28 \mu\text{m}$ at temperature 10 mK in GaAs [14] and $3 \mu\text{m}$ at temperature 30 mK in graphene [30]) is shorter than all the geometric lengths and that there is no bulk-leakage [13, 34, 52, 53]. Our classification, depicted in Table II, relies on both a qualitative distinction between auto- and cross-correlations, as well as quantitative differences. Our method applies for a uniform edge – moving away from this assumption, e.g. having puddles of Pf and APf separated by domain walls [42, 43], would require technique beyond ours. The many-puddle picture would facilitate heat leakage from the edge to the bulk [54]. As long as the measured two-terminal heat conductance is half-integer quantized, it weakens the

$\{\nu, \nu_i\}$	State	$ F_{1,2,c}^{\text{Full}} $	F_1^{Partial}	F_2^{Partial}	$ F_c^{\text{Partial}} $
$\{5/2, 2\}$	Pf	≈ 0	$= 0$	$= 0$	$= 0$
	APf	≈ 0.28	$= 0$	≈ 0.12 [34]	$= 0$
	PHPf	≈ 0	$= 0$	$= 0$	$= 0$
$\{5/2, 7/3\}$	Pf	≈ 0	≈ 0	≈ 0	≈ 0
	APf	≈ 0.25	≈ 0.5	≈ 0.5	≈ 0.27
	PHPf	≈ 0.11	≈ 0.26	≈ 0.26	≈ 0.26
$\{3, 5/2\}$	Pf	≈ 0.15	≈ 0.19	≈ 0.19	≈ 0.19
	APf	≈ 0	≈ 0.6	≈ 0.6	≈ 0.6
	PHPf	≈ 0	≈ 0	≈ 0	≈ 0

TABLE II. Summary of our results: F_1, F_2 are the auto-correlation Fano factors for the drains D_1, D_2 , respectively, and F_c is the cross-correlation Fano factor. For full thermal equilibration (fourth column) we have $F_1 = F_2 = |F_c| \equiv |F_{1,2,c}^{\text{Full}}|$. We use ≈ 0 to indicate exponential suppression as a function of the geometric lengths.

evidence for this non-uniform picture.

Device and thermal equilibration regimes.— Our device is made out of interfaces of the filling ν and filling $\nu_i (< \nu)$, c.f. Fig. 1. We choose $\{\nu, \nu_i\}$ as $\{5/2, 2\}$ or $\{5/2, 7/3\}$ or $\{3, 5/2\}$ and we assume $\nu_i = 7/3$ as an Abelian state [13–15, 55]. The relevant lengths for this device are (i) the internal characteristic lengths $l_{\text{eq}}^{\text{full}}$ and $l_{\text{eq}}^{\text{par}}$, and (ii) the geometric lengths L_{Arm} and L_{int} (cf. Fig. 1). $l_{\text{eq}}^{\text{full}}$ denotes the full thermal equilibration length (full equilibration has been observed over a distance $160 \mu\text{m}$ at temperature 11 mK in GaAs [15]), over which the heat transfer among all modes is fully facilitated, i.e., $l_{\text{eq}}^{\text{full}} \ll (L_{\text{Arm}}, L_{\text{int}})$ for full thermal equilibration. $l_{\text{eq}}^{\text{par}}$ denotes the partial thermal equilibration length, over which the heat transfer among modes of the same Landau level is fully facilitated but heat transfer among modes of different Landau Levels is negligible, i.e., $l_{\text{eq}}^{\text{par}} \ll (L_{\text{Arm}}, L_{\text{int}}) \ll l_{\text{eq}}^{\text{full}}$ for partial thermal equilibration. Equilibrated modes form a chiral hydrodynamic mode characterized by its electrical and thermal conductances. We refer to the direction parallel (anti-parallel) to the charge flow as downstream (upstream). We note that edge reconstruction cannot play any role in charge conductance due to full charge equilibration [30, 32, 33, 56]. For full thermal equilibration, each mode is equilibrated with other while for partial thermal equilibration, each mode is equilibrated with other only in a given Landau level. As edge reconstruction takes place in each Landau level, the effect of edge reconstruction is washed out in both the cases.

Heat transport and current-current correlations.— The thermal conductance of a hydrodynamic mode is determined by the difference of the thermal conductances of downstream and upstream modes (ν_Q) involved in the equilibration process. For $\nu_Q > 0$, $\nu_Q = 0$, or $\nu_Q < 0$, the nature of heat transport in that hydrodynamic mode

is, respectively, ballistic (B), diffusive (D), or antiballistic (AB) [52, 57]. For the B, D, and AB heat transport we have, respectively, exponentially suppressed, algebraically decaying, and constant CCC as a function of the geometric length of the mode [52, 57].

As contacts S and G in Fig. 2 are at different potentials, there are potential drops in the device which happen in the regions marked as hot spots, H_1, H_2 , resulting in Joule heating [57]. Two possible hot spots can also exist near the drains D_1, D_2 , though, heat generated there can not flow back to the middle region due to their specific configurations and hence can not contribute to the noise [57]. In addition, four noise spots (M, N, O, P) are formed due to the creation of thermally excited particle-hole pairs and their splitting into different drains D_1, D_2 (Fig. 2) [57]. CCC are computed by collecting the contributions from M, N, O, P . Let us elaborate on how the charge-neutral Majorana mode ψ contributes to CCC, as we know ψ alone cannot participate in particle-hole pair splitting. However, we can define a creation operator $\psi e^{\mp 2i\phi_{\pm}}$ (ϕ_{\pm} denotes downstream and upstream charge-1/2 boson, respectively) carrying an electron charge. As ψ always propagates alongside ϕ_{\pm} , they together can participate in particle-hole pair splitting.

The nature of heat transport in the “outer”, “line” and “upper” segments (cf. Fig. 1 and Fig. 2) determine the CCC [57–60]. We define a quantity ν_Q^{list} as [ν_Q in “outer”, ν_Q in “line”, ν_Q in “upper”]. In our analysis, ν_Q^{list} becomes either [B, B, B] or [B, AB, B] or [AB, AB, B] or [B, B, AB]. Hence, we have either exponentially suppressed or constant CCC as a function of the geometric lengths, which we use to discriminate among the states and their thermal equilibration regimes. For the [B, B, B] case the generated heat at H_1, H_2 flows downstream and reaches directly to the drains D_1, D_2 . Only an exponentially suppressed, $\mathcal{O}(\exp(-L_{\text{int}}/l_{\text{eq}}))$ and $\mathcal{O}(\exp(-L_{\text{Arm}}/l_{\text{eq}}))$, amount of heat reaches M, N and O, P with $l_{\text{eq}} = l_{\text{eq}}^{\text{full}}$ and $l_{\text{eq}} = l_{\text{eq}}^{\text{par}}$ for full and partial thermal equilibrations, respectively. Therefore an exponentially suppressed CCC is found. For the [B, AB, B] and [B, B, AB] cases the generated heat at H_1, H_2 flows upstream along the “line” and “upper” segments, respectively. Thus, M, N provide constant contributions to the CCC, but the amount of heat that reaches O, P is exponentially suppressed. For the [AB, AB, B] case the generated heat at H_1, H_2 flows upstream along both the “line” and “outer” segments. Thus both M, N and O, P provide constant contributions to CCC [61]. For partial thermal equilibration, we treat the lowest and second Landau levels dis-jointly while computing CCC. Given impurity-facilitated inter-mode tunneling as well as inter-mode interaction, equivalent (yet counter-propagating in ν and ν_i) lowest Landau level modes become localized, decoupling them from the transport processes along the “line”. Hence, the modes in the lowest Landau level do not contribute to CCC, while the modes in the second

Landau level do contribute.

Let us denote by I_1 and I_2 the currents entering the drains D_1 and D_2 , respectively. The corresponding current-current auto-correlations are defined as $\delta^2 I_1 = \langle (I_1 - \langle I_1 \rangle)^2 \rangle$ in D_1 and $\delta^2 I_2 = \langle (I_2 - \langle I_2 \rangle)^2 \rangle$ in D_2 , while the cross-correlation is $\delta^2 I_c = \langle (I_1 - \langle I_1 \rangle)(I_2 - \langle I_2 \rangle) \rangle$ [62]. The corresponding Fano factors are defined as $F_j = |\delta^2 I_j|/2e\langle I \rangle t(1-t)$, with $j \in \{1, 2, c\}$, where I is the source current and $t = \langle I_1 \rangle / \langle I \rangle$. The Fano factors are found to be [63] $F_1 = F_2 = F_O + F_P + F_M + F_N$ and $F_c = F'_O + F'_P - F_M - F_N$, where F_{α} is the contribution to the auto-correlations from the noise spot $\alpha \in \{M, N, O, P\}$ and F'_{β} is the contribution to the cross-correlation from the noise spot $\beta \in \{O, P\}$. We evaluate these contributions as

$$\begin{aligned} 2eIt(1-t)(F_M + F_N) &= 2\frac{e^2}{h}(\nu - \nu_i)\frac{\nu_i}{\nu}k_B(T_M + T_N), \\ 2eIt(1-t)(F_O + F_P) &= \frac{1}{\nu^2}(\nu_i^2 S_O + (\nu - \nu_i)^2 S_P), \\ 2eIt(1-t)(F'_O + F'_P) &= \frac{\nu_i(\nu - \nu_i)}{\nu^2}(S_O + S_P), \end{aligned} \quad (1)$$

where k_B is the Boltzmann constant, and we obtain the temperatures $T_M = T_N$ at M, N by solving self-consistent equilibration equations and considering energy conservations [57, 63]. We find the noise contributions $S_O = S_P$ by computing [57, 63]

$$S_O = S_P = \frac{2e^2}{h} \frac{\nu' \nu_-}{l_{\text{eq}}^{\text{ch}} \nu_+} \int_0^{L_{\text{Arm}}} \frac{e^{-\frac{2x}{l_{\text{eq}}^{\text{ch}}}} k_B [T_+(x) + T_-(x)] dx}{l_{\text{eq}}^{\text{ch}} \left[1 - \left(e^{-\frac{L_{\text{Arm}}}{l_{\text{eq}}^{\text{ch}}}} \frac{\nu_-}{\nu_+} \right)^2 \right]^2} \quad (2)$$

in the limit $l_{\text{eq}} \ll L_{\text{Arm}}$, where $\nu' = (\nu_+ - \nu_-)$. Here $l_{\text{eq}}^{\text{ch}}$ is the charge equilibration length, and $T_{\pm}(x)$ (which depend on l_{eq}) are the temperature profiles in ν_{\pm} , where ν_+ and ν_- are the filling factors of the downstream and the upstream mode in the “outer” segment, respectively. $T_{\pm}(x)$ are calculated by solving the equations of heat equilibration under the assumptions that no voltage drop occurs along the “outer” segment and the lead contacts are at zero temperature. We note that in some cases we also have *qualitative differences* between the auto-correlation and cross-correlation Fano factors apart from their quantitative differences (see Table II).

The case $\{\nu, \nu_i\} = \{5/2, 2\}$.—

(a) Full thermal equilibration.— For the Pf and PHPf states we have $\nu_Q^{\text{list}} = [7/2, 3/2, 2]$ and $\nu_Q^{\text{list}} = [5/2, 1/2, 2]$, respectively. The nature of heat transport is [B, B, B] for both states resulting in exponentially suppressed CCC. For the APf state we have $\nu_Q^{\text{list}} = [3/2, -1/2, 2]$, thus the nature of heat transport is [B, AB, B]. In this case $F_O + F_P, F'_O + F'_P$ are exponentially suppressed and $F_M + F_N$

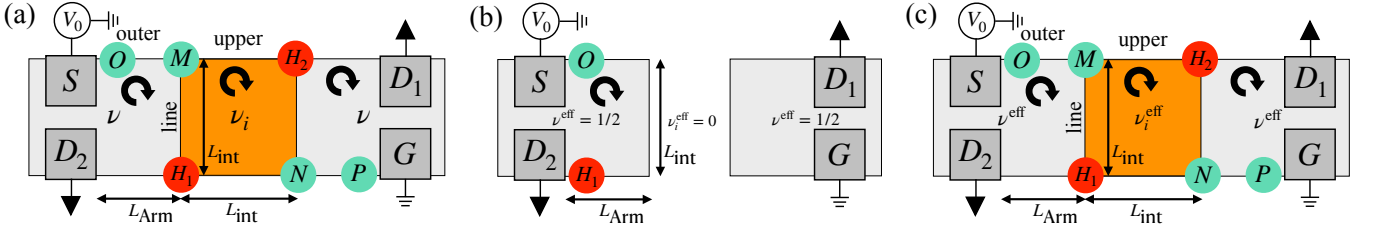


FIG. 2. Noise generation in our proposed device (see Fig. 1) for full (a) and partial (b,c) thermal equilibration, where in the latter scenario the modes in the lowest Landau level localize in the “line” segment. Each circular arrow indicates the chirality of charge propagation of the respective filling. Voltage drops occur at the hot spots H_1, H_2 (red circles), resulting in the noise spots M, N, O, P (green circles) [57]. In (a) we have $\{\nu, \nu_i\}$ as $\{5/2, 2\}$ or $\{5/2, 7/3\}$ or $\{3, 5/2\}$. In (b) we effectively have the filling $\{\nu^{\text{eff}}, \nu_i^{\text{eff}}\} = \{1/2, 0\}$ for $\{\nu, \nu_i\} = \{5/2, 2\}$. In (c) we effectively have the filling $\{\nu^{\text{eff}}, \nu_i^{\text{eff}}\} = \{1/2, 1/3\}$ for $\{\nu, \nu_i\} = \{5/2, 7/3\}$ and $\{\nu^{\text{eff}}, \nu_i^{\text{eff}}\} = \{1, 1/2\}$ for $\{\nu, \nu_i\} = \{3, 5/2\}$.

provides a constant contribution, leading to $F_1 = F_2 = |F_c| \neq 0$ (Table II and [63]).

(b) Partial thermal equilibration.— The modes in the second Landau level equilibrate and form a hydrodynamic mode connecting S, D_2 and G, D_1 individually. Since only S is biased, CCC can only appear in D_2 , hence $F_1 = |F_c| = 0$ always. For the Pf and PHPf states we have $\nu_Q = 3/2$ and $\nu_Q = 1/2$ for the mode connecting S, D_2 leading to the ballistic heat transport and an exponentially suppressed CCC. For the APf state we have $\nu_Q = -1/2$ for the mode connecting S, D_2 leading to antiballistic heat transport and a constant CCC ($F_2 \neq 0$) (Table II and [34]).

The case $\{\nu, \nu_i\} = \{5/2, 7/3\}$.—

(a) Full thermal equilibration.— For the Pf state we have $\nu_Q^{\text{list}} = [7/2, 1/2, 3]$. The nature of heat transport is [B, B, B], thus CCC are exponentially suppressed. For the APf and PHPf states we have $\nu_Q^{\text{list}} = [3/2, -3/2, 3]$ and $\nu_Q^{\text{list}} = [5/2, -1/2, 3]$, respectively. The nature of heat transport is [B, AB, B] for both the APf and PHPf states. In these cases $F_O + F_P, F'_O + F'_P$ are exponentially suppressed and $F_M + F_N$ provides a constant contribution to the CCC, leading to $F_1 = F_2 = |F_c| \neq 0$ (Table II and [63]).

(b) Partial thermal equilibration.— For the Pf state we have $\nu_Q^{\text{list}} = [3/2, 1/2, 1]$. The nature of heat transport is [B, B, B], thus CCC is exponentially suppressed. For the APf state we have $\nu_Q^{\text{list}} = [-1/2, -3/2, 1]$. The nature of heat transport is then [AB, AB, B], hence $F_O + F_P, F'_O + F'_P, F_M + F_N$ all provide constant contributions, leading to $F_1 = F_2 > |F_c| \neq 0$ (Table II and [63]). For the PHPf state we have $\nu_Q^{\text{list}} = [1/2, -1/2, 1]$. The nature of heat transport is therefore [B, AB, B]. In this case $F_O + F_P, F'_O + F'_P$ are exponentially suppressed and $F_M + F_N$ provides a constant contribution to the CCC, leading to $F_1 = F_2 = |F_c| \neq 0$ (Table II and [63]).

The case $\{\nu, \nu_i\} = \{3, 5/2\}$.—

(a) Full thermal equilibration.— For the Pf state we have $\nu_Q^{\text{list}} = [3, -1/2, 7/2]$. The nature of heat transport is [B, AB, B]. In this case $F_O + F_P, F'_O + F'_P$ are expo-

ponentially suppressed and $F_M + F_N$ provides a constant contribution to the CCC, leading to $F_1 = F_2 = |F_c| \neq 0$ (Table II and [63]). For the APf and PHPf states we have $\nu_Q^{\text{list}} = [3, 3/2, 3/2]$ and $\nu_Q^{\text{list}} = [3, 1/2, 5/2]$. The nature of heat transport is [B, B, B] for both states, thus CCC are exponentially suppressed.

(b) Partial thermal equilibration.— For the Pf and APf states we have $\nu_Q^{\text{list}} = [1, -1/2, 3/2]$ and $\nu_Q^{\text{list}} = [1, 3/2, -1/2]$, respectively, thus the nature of heat transports are [B, AB, B] and [B, B, AB], respectively. In each case $F_O + F_P, F'_O + F'_P$ are exponentially suppressed and $F_M + F_N$ provides a constant contribution to the CCC, leading to $F_1 = F_2 = |F_c| \neq 0$ (Table II and [63]). For the PHPf state we have $\nu_Q^{\text{list}} = [1, 1/2, 1/2]$, leading to the nature of heat transport as [B, B, B], thus CCC are exponentially suppressed.

Protocol.— Based on our results (Table II), we now present a sequential protocol to distinguish both the bulk Pf, APf, and PHPf states and the regimes of thermal equilibration: full vs. partial. First we choose $\{\nu, \nu_i\} = \{5/2, 2\}$ and measure F_1, F_2, F_c . If $F_2 \neq 0$ then the state is APf. If in addition $F_1 = F_2 = |F_c| \neq 0$ then we have full thermal equilibration, while if $F_1 = |F_c| = 0$ then we have partial thermal equilibration. If on the other hand $F_1 = F_2 = |F_c| = 0$, then the state can be either Pf or PHPf. Next we choose $\{\nu, \nu_i\} = \{5/2, 7/3\}$. If $F_1 = F_2 = |F_c| \neq 0$ then the state is PHPf. We can distinguish between the full and partial thermal equilibration regimes via the change in the Fano factors. If $F_1 = F_2 = |F_c| = 0$, then the state is Pf. Thereafter, we choose $\{\nu, \nu_i\} = \{3, 5/2\}$. The value of $F_1 = F_2 = |F_c| \neq 0$ distinguish between the full or partial thermal equilibration regimes. We mention that, in principle, one can employ our method to distinguish among the $SU(2)_2$ family members (by suitably choosing $\{\nu, \nu_i\}$) [29], which are, however, inconsistent with experimental measurements [13–15].

Summary and outlook.— We have considered a device comprising of the interface between the 5/2 state with an Abelian state. We have considered the Pf, APf,

and PHPf states. We have studied both the full and partial thermal equilibration regimes, where heat transfer among different Landau Levels is, respectively, fully facilitated or negligible. Throughout our analysis, the effective electro-chemical potential of the various edge modes is assumed to be fully equilibrated, leading to full charge equilibration [30–33]. Our CCC-based protocol provides a new platform, different than other experimental platforms, capable of distinguishing among the Pf, APf, and PHPf states along with their thermal equilibration regimes: full vs. partial (see Table II). Despite of challenges and limitations to the experimental implementation, we note that we just need two interfaces for making this device and one can tune the filling in the middle region by changing the gate voltage. Various experiments have already implemented devices based on interfaces both in GaAs [14, 15, 56, 64, 65] and in graphene [66–68].

The application of the idea outlined here goes beyond the $5/2$ non-Abelian state in GaAs, for example classifying the $12/5$ state [69–73] and other Abelian states [58–60] in GaAs. They can also be extended to graphene [74–77] quantum Hall. Another interesting possibility is to study the non-Abelian phase of α -RuCl₃ Kitaev magnet [78–80].

We thank Alexander D. Mirlin, Bivas Dutta, Christian Spånslätt, Jinhong Park, Kun Yang, Matthew Foster, Moty Heiblum, Nandini Trivedi, and Subir Sachdev for useful discussions. This research was supported in part by the International Centre for Theoretical Sciences (ICTS) for participating in the program - Condensed Matter meets Quantum Information (code: ICTS/COMQUI2023/9). S.M. was supported by Weizmann Institute of Science, Israel Deans fellowship through Feinberg Graduate School and the Raymond and Beverly Sackler Center for Computational Molecular and Material Science at Tel Aviv University. A.D. was supported by the German-Israeli Foundation Grant No. I-1505-303.10/2019, DFG MI 658/10-2, DFG RO 2247/11-1, DFG EG 96/13-1, and CRC 183 (project C01). A.D. also thanks the Israel planning and budgeting committee (PBC) and the Weizmann Institute of Science, the Dean of Faculty fellowship, and the Koshland Foundation for financial support. M.G. has been supported by the Israel Science Foundation (ISF) and the Directorate for Defense Research and Development (DDR&D) Grant No. 3427/21 and by the US-Israel Binational Science Foundation (BSF) Grant No. 2020072. Y.G. acknowledges support by the DFG Grant MI 658/10-2, by the German-Israeli Foundation Grant I-1505-303.10/2019, by the Helmholtz International Fellow Award, by the DFG Grant RO 2247/11-1, by CRC 183 (project C01), and by the Minerva Foundation.

S.M. and A.D. contributed equally to this work.

* sourav.manna@weizmann.ac.il

† ankur.das@weizmann.ac.il

- [1] G. Moore and N. Read, Nonabelions in the fractional quantum hall effect, *Nuclear Physics B* **360**, 362 (1991).
- [2] T. I. Andersen et. al., Observation of non-abelian exchange statistics on a superconducting processor, [arXiv:2210.10255](https://arxiv.org/abs/2210.10255) (2022).
- [3] R. Willett, J. P. Eisenstein, H. L. Störmer, D. C. Tsui, A. C. Gossard, and J. H. English, Observation of an even-denominator quantum number in the fractional quantum hall effect, *Phys. Rev. Lett.* **59**, 1776 (1987).
- [4] K. K. W. Ma, M. R. Peterson, V. W. Scarola, and K. Yang, Fractional quantum hall effect at the filling factor $\nu = 5/2$, [arXiv:2208.07908](https://arxiv.org/abs/2208.07908) (2022).
- [5] S.-S. Lee, S. Ryu, C. Nayak, and M. P. A. Fisher, Particle-hole symmetry and the $\nu = \frac{5}{2}$ quantum hall state, *Phys. Rev. Lett.* **99**, 236807 (2007).
- [6] M. Levin, B. I. Halperin, and B. Rosenow, Particle-hole symmetry and the pfaffian state, *Phys. Rev. Lett.* **99**, 236806 (2007).
- [7] L. Fidkowski, X. Chen, and A. Vishwanath, Non-abelian topological order on the surface of a 3d topological superconductor from an exactly solved model, *Phys. Rev. X* **3**, 041016 (2013).
- [8] D. T. Son, Is the composite fermion a dirac particle?, *Phys. Rev. X* **5**, 031027 (2015).
- [9] P. T. Zucker and D. E. Feldman, Stabilization of the particle-hole pfaffian order by landau-level mixing and impurities that break particle-hole symmetry, *Phys. Rev. Lett.* **117**, 096802 (2016).
- [10] L. Antonić, J. Vučičević, and M. V. Milovanović, Paired states at $5/2$: Particle-hole pfaffian and particle-hole symmetry breaking, *Phys. Rev. B* **98**, 115107 (2018).
- [11] R. V. Mishmash, D. F. Mross, J. Alicea, and O. I. Motrunich, Numerical exploration of trial wave functions for the particle-hole-symmetric pfaffian, *Phys. Rev. B* **98**, 081107 (2018).
- [12] E. H. Rezayi, K. Pakrouski, and F. D. M. Haldane, Stability of the particle-hole pfaffian state and the $\frac{5}{2}$ -fractional quantum hall effect, *Phys. Rev. B* **104**, L081407 (2021).
- [13] M. Banerjee, M. Heiblum, V. Umansky, D. E. Feldman, Y. Oreg, and A. Stern, Observation of half-integer thermal hall conductance, *Nature* **559**, 205 (2018).
- [14] B. Dutta, W. Yang, R. Melcer, H. K. Kundu, M. Heiblum, V. Umansky, Y. Oreg, A. Stern, and D. Mross, Distinguishing between non-abelian topological orders in a quantum hall system, *Science* **375**, 193 (2022).
- [15] B. Dutta, V. Umansky, M. Banerjee, and M. Heiblum, Isolated ballistic non-abelian interface channel, *Science* **377**, 1198 (2022).
- [16] R. H. Morf, Transition from quantum hall to compressible states in the second landau level: New light on the $\nu = 5/2$ enigma, *Phys. Rev. Lett.* **80**, 1505 (1998).
- [17] E. H. Rezayi and F. D. M. Haldane, Incompressible paired hall state, stripe order, and the composite fermion liquid phase in half-filled landau levels, *Phys. Rev. Lett.* **84**, 4685 (2000).

- [18] M. R. Peterson, T. Jolicoeur, and S. Das Sarma, Finite-layer thickness stabilizes the pfaffian state for the $5/2$ fractional quantum hall effect: Wave function overlap and topological degeneracy, *Phys. Rev. Lett.* **101**, 016807 (2008).
- [19] A. Wójs, C. Tóke, and J. K. Jain, Landau-level mixing and the emergence of pfaffian excitations for the $5/2$ fractional quantum hall effect, *Phys. Rev. Lett.* **105**, 096802 (2010).
- [20] M. Storni, R. H. Morf, and S. Das Sarma, Fractional quantum hall state at $\nu = \frac{5}{2}$ and the moore-read pfaffian, *Phys. Rev. Lett.* **104**, 076803 (2010).
- [21] E. H. Rezayi and S. H. Simon, Breaking of particle-hole symmetry by landau level mixing in the $\nu = 5/2$ quantized hall state, *Phys. Rev. Lett.* **106**, 116801 (2011).
- [22] K. Pakrouski, M. R. Peterson, T. Jolicoeur, V. W. Scarola, C. Nayak, and M. Troyer, Phase diagram of the $\nu = 5/2$ fractional quantum hall effect: Effects of landau-level mixing and nonzero width, *Phys. Rev. X* **5**, 021004 (2015).
- [23] A. E. Feiguin, E. Rezayi, C. Nayak, and S. Das Sarma, Density matrix renormalization group study of incompressible fractional quantum hall states, *Phys. Rev. Lett.* **100**, 166803 (2008).
- [24] A. E. Feiguin, E. Rezayi, K. Yang, C. Nayak, and S. Das Sarma, Spin polarization of the $\nu = 5/2$ quantum hall state, *Phys. Rev. B* **79**, 115322 (2009).
- [25] B. Halperin, Theory of the quantized hall conductance, *Helv. Phys. Acta* **56**, 75 (1983).
- [26] G. Yang and D. E. Feldman, Experimental constraints and a possible quantum hall state at $\nu = 5/2$, *Phys. Rev. B* **90**, 161306 (2014).
- [27] G. Yang and D. E. Feldman, Influence of device geometry on tunneling in the $\nu = \frac{5}{2}$ quantum hall liquid, *Phys. Rev. B* **88**, 085317 (2013).
- [28] X. G. Wen, Non-abelian statistics in the fractional quantum hall states, *Phys. Rev. Lett.* **66**, 802 (1991).
- [29] J. K. Jain, Incompressible quantum hall states, *Phys. Rev. B* **40**, 8079 (1989).
- [30] S. K. Srivastav, R. Kumar, C. Spånslätt, K. Watanabe, T. Taniguchi, A. D. Mirlin, Y. Gefen, and A. Das, Vanishing thermal equilibration for hole-conjugate fractional quantum hall states in graphene, *Phys. Rev. Lett.* **126**, 216803 (2021).
- [31] R. A. Melcer, B. Dutta, C. Spånslätt, J. Park, A. D. Mirlin, and V. Umansky, Absent thermal equilibration on fractional quantum hall edges over macroscopic scale, *Nature Communications* **13**, 376 (2022).
- [32] R. Kumar, S. K. Srivastav, C. Spånslätt, K. Watanabe, T. Taniguchi, Y. Gefen, A. D. Mirlin, and A. Das, Observation of ballistic upstream modes at fractional quantum hall edges of graphene, *Nature Communications* **13**, 213 (2022).
- [33] S. K. Srivastav, R. Kumar, C. Spånslätt, K. Watanabe, T. Taniguchi, A. D. Mirlin, Y. Gefen, and A. Das, Determination of topological edge quantum numbers of fractional quantum hall phases by thermal conductance measurements, *Nature Communications* **13**, 5185 (2022).
- [34] J. Park, C. Spånslätt, Y. Gefen, and A. D. Mirlin, Noise on the non-abelian $\nu = 5/2$ fractional quantum hall edge, *Phys. Rev. Lett.* **125**, 157702 (2020).
- [35] M. Heiblum (unpublished); M. Yutushui, A. Stern, and D. F. Mross, Identifying the $\nu = \frac{5}{2}$ topological order through charge transport measurements, *Phys. Rev. Lett.* **128**, 016401 (2022).
- [36] M. Hein and C. Spånslätt, Thermal conductance and noise of majorana modes along interfaced $\nu = 5/2$ fractional quantum hall states, [arXiv:2211.08000](https://arxiv.org/abs/2211.08000) (2022).
- [37] D. E. Feldman and F. Li, Charge-statistics separation and probing non-abelian states, *Phys. Rev. B* **78**, 161304 (2008).
- [38] H.-H. Lai and K. Yang, Distinguishing particle-hole conjugated fractional quantum hall states using quantum-dot-mediated edge transport, *Phys. Rev. B* **87**, 125130 (2013).
- [39] X. Wan and K. Yang, Striped quantum hall state in a half-filled landau level, *Phys. Rev. B* **93**, 201303 (2016).
- [40] S. H. Simon, Interpretation of thermal conductance of the $\nu = 5/2$ edge, *Phys. Rev. B* **97**, 121406 (2018).
- [41] B. Lian and J. Wang, Theory of the disordered $\nu = \frac{5}{2}$ quantum thermal hall state: Emergent symmetry and phase diagram, *Phys. Rev. B* **97**, 165124 (2018).
- [42] C. Wang, A. Vishwanath, and B. I. Halperin, Topological order from disorder and the quantized hall thermal metal: Possible applications to the $\nu = 5/2$ state, *Phys. Rev. B* **98**, 045112 (2018).
- [43] D. F. Mross, Y. Oreg, A. Stern, G. Margalit, and M. Heiblum, Theory of disorder-induced half-integer thermal hall conductance, *Phys. Rev. Lett.* **121**, 026801 (2018).
- [44] D. E. Feldman, Comment on “interpretation of thermal conductance of the $\nu = 5/2$ edge”, *Phys. Rev. B* **98**, 167401 (2018).
- [45] K. K. W. Ma and D. E. Feldman, Partial equilibration of integer and fractional edge channels in the thermal quantum hall effect, *Phys. Rev. B* **99**, 085309 (2019).
- [46] S. H. Simon, M. Ippoliti, M. P. Zaletel, and E. H. Rezayi, Energetics of pfaffian-anti-pfaffian domains, *Phys. Rev. B* **101**, 041302 (2020).
- [47] H. Asasi and M. Mulligan, Partial equilibration of anti-pfaffian edge modes at $\nu = 5/2$, *Phys. Rev. B* **102**, 205104 (2020).
- [48] W. Zhu, D. N. Sheng, and K. Yang, Topological interface between pfaffian and anti-pfaffian order in $\nu = 5/2$ quantum hall effect, *Phys. Rev. Lett.* **125**, 146802 (2020).
- [49] P.-S. Hsin, Y.-H. Lin, N. M. Paquette, and J. Wang, Effective field theory for fractional quantum hall systems near $\nu = 5/2$, *Phys. Rev. Research* **2**, 043242 (2020).
- [50] S. H. Simon and B. Rosenow, Partial equilibration of the anti-pfaffian edge due to majorana disorder, *Phys. Rev. Lett.* **124**, 126801 (2020).
- [51] F. D. M. Haldane, E. H. Rezayi, and K. Yang, Graviton chirality and topological order in the half-filled landau level, *Phys. Rev. B* **104**, L121106 (2021).
- [52] C. Spånslätt, J. Park, Y. Gefen, and A. D. Mirlin, Topological classification of shot noise on fractional quantum hall edges, *Phys. Rev. Lett.* **123**, 137701 (2019).
- [53] A. Aharon-Steinberg, Y. Oreg, and A. Stern, Phenomenological theory of heat transport in the fractional quantum hall effect, *Phys. Rev. B* **99**, 041302 (2019).
- [54] R. A. Melcer, A. Gil, A.-K. Paul, P. Tiwary, V. Umansky, M. Heiblum, Y. Oreg, A. Stern, and E. Berg, Heat conductance of the quantum hall bulk, [arXiv:2306.14977](https://arxiv.org/abs/2306.14977) (2023).
- [55] M. Dolev, Y. Gross, R. Sabo, I. Gurman, M. Heiblum, V. Umansky, and D. Mahalu, Characterizing neutral modes of fractional states in the second landau level, *Phys. Rev. Lett.* **107**, 036805 (2011).

- [56] Y. Cohen, Y. Ronen, W. Yang, D. Banitt, J. Park, M. Heiblum, A. D. Mirlin, Y. Gefen, and V. Umansky, Synthesizing a $\nu=2/3$ fractional quantum hall effect edge state from counter-propagating $\nu=1$ and $\nu=1/3$ states, *Nature Communications* **10**, 1920 (2019).
- [57] C. Spänslätt, J. Park, Y. Gefen, and A. D. Mirlin, Conductance plateaus and shot noise in fractional quantum hall point contacts, *Phys. Rev. B* **101**, 075308 (2020).
- [58] S. Manna, A. Das, and M. Goldstein, Shot noise as a diagnostic in the fractional quantum hall edge zoo, [arXiv:2307.05173](https://arxiv.org/abs/2307.05173) (2023).
- [59] S. Manna, A. Das, and M. Goldstein, Shot noise classification of different conductance plateaus in a quantum point contact at the $\nu = 2/3$ edge, [arXiv:2307.05175](https://arxiv.org/abs/2307.05175) (2023).
- [60] S. Manna and A. Das, Experimentally motivated order of length scales affect shot noise, [arXiv:2307.08264](https://arxiv.org/abs/2307.08264) (2023).
- [61] In the partial thermal equilibration regime, algebraic corrections, $\mathcal{O}(\sqrt{L_{\text{Arm}}/l_{\text{eq}}^{\text{full}}})$ and $\mathcal{O}(\sqrt{L_{\text{int}}/l_{\text{eq}}^{\text{full}}})$, to the CCC originate due to weak heat loss from the second Landau level to the lowest Landau level [34]. In the limit $l_{\text{eq}}^{\text{par}} \ll (L_{\text{Arm}}, L_{\text{int}}) \ll l_{\text{eq}}^{\text{full}}$, these corrections become negligible.
- [62] We define the time average of an operator x as $\langle x \rangle = \lim_{\tau \rightarrow \infty} \frac{1}{\tau} \int_{-\tau}^{\tau} x(t) dt$.
- [63] See the supplementary material for technical details of the calculations.
- [64] S. Biswas, R. Bhattacharyya, H. K. Kundu, A. Das, M. Heiblum, V. Umansky, M. Goldstein, and Y. Gefen, Shot noise does not always provide the quasiparticle charge, *Nature Physics* **18**, 1476 (2022).
- [65] M. Hashisaka, T. Ito, T. Akiho, S. Sasaki, N. Kumada, N. Shibata, and K. Muraki, Coherent-incoherent crossover of charge and neutral mode transport as evidence for the disorder-dominated fractional edge phase, [arXiv:2212.13399](https://arxiv.org/abs/2212.13399) (2022).
- [66] C. Kumar, M. Kuiri, and A. Das, Equilibration of quantum hall edge states and its conductance fluctuations in graphene p-n junctions, *Solid State Communications* **270**, 38 (2018).
- [67] C. Kumar, S. K. Srivastav, and A. Das, Equilibration of quantum hall edges in symmetry-broken bilayer graphene, *Phys. Rev. B* **98**, 155421 (2018).
- [68] A. K. Paul, M. R. Sahu, K. Watanabe, T. Taniguchi, J. K. Jain, G. Murthy, and A. Das, Electrically switchable tunneling across a graphene pn junction: evidence for canted antiferromagnetic phase in $\nu = 0$ state, [arXiv:2205.00710](https://arxiv.org/abs/2205.00710) (2022).
- [69] N. Read and E. Rezayi, Beyond paired quantum hall states: Parafermions and incompressible states in the first excited landau level, *Phys. Rev. B* **59**, 8084 (1999).
- [70] W. Bishara, G. A. Fiete, and C. Nayak, Quantum hall states at $\nu = \frac{2}{k+2}$: Analysis of the particle-hole conjugates of the general level- k read-rezayi states, *Phys. Rev. B* **77**, 241306 (2008).
- [71] J. S. Xia, W. Pan, C. L. Vicente, E. D. Adams, N. S. Sullivan, H. L. Stormer, D. C. Tsui, L. N. Pfeiffer, K. W. Baldwin, and K. W. West, Electron correlation in the second landau level: A competition between many nearly degenerate quantum phases, *Phys. Rev. Lett.* **93**, 176809 (2004).
- [72] A. Kumar, G. A. Csáthy, M. J. Manfra, L. N. Pfeiffer, and K. W. West, Nonconventional odd-denominator fractional quantum hall states in the second landau level, *Phys. Rev. Lett.* **105**, 246808 (2010).
- [73] P. Bonderson and J. K. Slingerland, Fractional quantum hall hierarchy and the second landau level, *Phys. Rev. B* **78**, 125323 (2008).
- [74] J. I. Li, C. Tan, S. Chen, Y. Zeng, T. Taniguchi, K. Watanabe, J. Hone, and C. R. Dean, Even-denominator fractional quantum hall states in bilayer graphene, *Science* **358**, 648 (2017).
- [75] K. Huang, H. Fu, D. R. Hickey, N. Alem, X. Lin, K. Watanabe, T. Taniguchi, and J. Zhu, Valley isospin controlled fractional quantum hall states in bilayer graphene, *Phys. Rev. X* **12**, 031019 (2022).
- [76] D.-K. Ki, V. I. Fal'ko, D. A. Abanin, and A. F. Morpurgo, Observation of even denominator fractional quantum hall effect in suspended bilayer graphene, *Nano Letters* **14**, 2135 (2014).
- [77] A. A. Zibrov, C. Kometter, H. Zhou, E. M. Spanton, T. Taniguchi, K. Watanabe, M. P. Zaletel, and A. F. Young, Tunable interacting composite fermion phases in a half-filled bilayer-graphene landau level, *Nature* **549**, 360 (2017).
- [78] A. Banerjee, C. A. Bridges, J. Q. Yan, A. A. Aczel, L. Li, M. B. Stone, G. E. Granroth, M. D. Lumsden, Y. Yiu, J. Knolle, S. Bhattacharjee, D. L. Kovrizhin, R. Moessner, D. A. Tennant, D. G. Mandrus, and S. E. Nagler, Proximate kitaev quantum spin liquid behaviour in a honeycomb magnet, *Nature Materials* **15**, 733 (2016).
- [79] Y. Kasahara, T. Ohnishi, Y. Mizukami, O. Tanaka, S. Ma, K. Sugii, N. Kurita, H. Tanaka, J. Nasu, Y. Motome, T. Shibauchi, and Y. Matsuda, Majorana quantization and half-integer thermal quantum hall effect in a kitaev spin liquid, *Nature* **559**, 227 (2018).
- [80] A. Kitaev, Anyons in an exactly solved model and beyond, *Annals of Physics* **321**, 2 (2006).

Supplemental material for: “Full Classification of Transport on an Equilibrated 5/2 Edge via Shot Noise”

Sourav Manna,^{1,2} Ankur Das,¹ Moshe Goldstein,² and Yuval Gefen¹

¹*Department of Condensed Matter Physics, Weizmann Institute of Science, Rehovot 7610001, Israel*

²*Raymond and Beverly Sackler School of Physics and Astronomy, Tel-Aviv University, Tel Aviv 6997801, Israel*

The supplemental material contains the following details:

1. Proposed device and configurations and general expression for the current-current correlations (CCC) in Section SI.
2. Expressions for the CCC for three specific cases of edge equilibrations in the device in Section SII.
3. CCC values for specific cases with Pfaffian (Pf), anti-Pf (APf), and particle-hole-Pf (PHPf) states in different configurations in Section SIII.

SI. DEVICE AND GENERAL EXPRESSION OF CCC

In this section we re-describe our proposed device in Section SIA to facilitate the follow up discussions for the readers. In Section SIB we derive general expression for the CCC in our device.

A. Proposed device

Our device is a Hall bar with filling ν and a depleted middle region with filling $\nu_i (< \nu)$, c.f. Fig. S1. We choose $\{\nu, \nu_i\}$ as $\{5/2, 2\}$ or $\{5/2, 7/3\}$ or $\{3, 5/2\}$. We have a source contact S which is biased by a dc voltage V_0 , a ground contact G , and two drains D_1, D_2 .

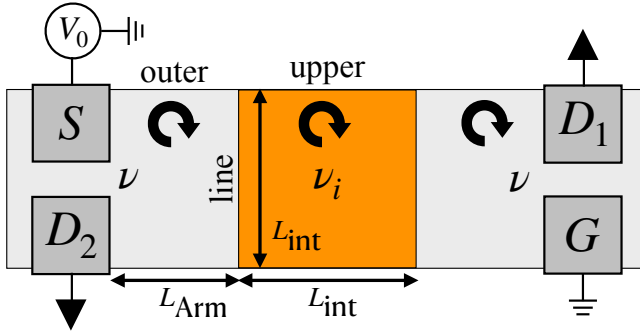


FIG. S1. Our proposed device (same as in main text): A Hall bar with filling ν with the middle region depleted to $\nu_i (< \nu)$. This creates two interfaces (“line”). We choose $\{\nu, \nu_i\}$ as $\{5/2, 2\}$ or $\{5/2, 7/3\}$ or $\{3, 5/2\}$. We also have the boundary of the vacuum with ν (“outer”) and with ν_i (“upper”). There are four contacts: a source S (biased by a dc voltage V_0), a ground G , and two drains D_1, D_2 . Each circular arrow indicates the chirality of charge propagation of the respective filling. L_{Arm} and L_{int} , the geometric lengths, are assumed to be of the same order of magnitude.

B. General expression for the CCC

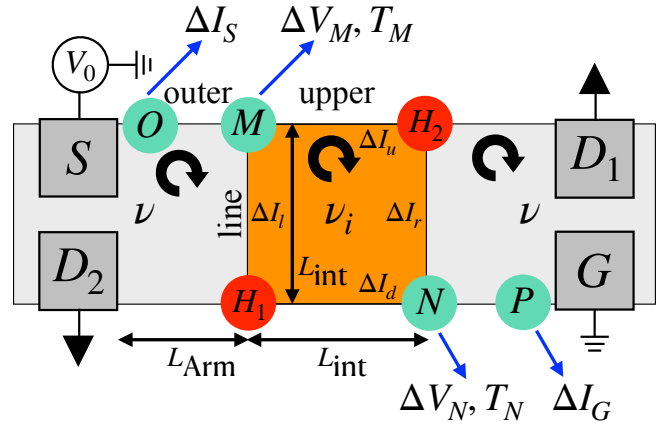


FIG. S2. Noise generation in our proposed device (see Fig. S1), where charge and heat are equilibrated in each segment. Each circular arrow shows the chirality of charge propagation of the respective filling. Voltage drops occur at the hot spots H_1, H_2 (red circles), resulting in noise spots M, N, O, P (green circles) [1]. The current fluctuations ΔI_S and ΔI_G are at O and P , respectively. We denote fluctuations in the local voltages at the noise spots M and N by ΔV_M and ΔV_N , respectively. The temperatures at the noise spots M and N are T_M and T_N , respectively. We denote the current fluctuations in the segments of the middle region, with filling ν_i , as $\Delta I_u, \Delta I_d, \Delta I_l, \Delta I_r$.

Let us denote by I_1 and I_2 the currents entering the drains D_1 and D_2 , respectively (Fig. S2). The corresponding current-current auto-correlations are defined as $\delta^2 I_1 = \langle (I_1 - \langle I_1 \rangle)^2 \rangle$ in D_1 and $\delta^2 I_2 = \langle (I_2 - \langle I_2 \rangle)^2 \rangle$ in D_2 , while the cross-correlation is $\delta^2 I_c = \langle (I_1 - \langle I_1 \rangle)(I_2 - \langle I_2 \rangle) \rangle$, where we define the time average of an operator x as $\langle x \rangle = \lim_{\tau \rightarrow \infty} \frac{1}{\tau} \int_{-\tau}^{\tau} x(t) dt$. We consult Fig. S2 and follow Ref. [1] to write

$$\begin{aligned} (I_1 - \langle I_1 \rangle) &= \Delta I_u + \Delta I_r, \\ (I_2 - \langle I_2 \rangle) &= \Delta I_d + \Delta I_l. \end{aligned} \quad (\text{S1})$$

The current fluctuations $\Delta I_u, \Delta I_d, \Delta I_l, \Delta I_r$, are composed of the voltage fluctuations, $\Delta V_M, \Delta V_N$, and the

thermal fluctuations $\Delta I_u^{\text{th}}, \Delta I_d^{\text{th}}, \Delta I_l^{\text{th}}, \Delta I_r^{\text{th}}$. We write

$$\begin{aligned}\Delta I_l &= (\nu - \nu_i) \frac{e^2}{h} \Delta V_M + \Delta I_l^{\text{th}}, \\ \Delta I_u &= \nu_i \frac{e^2}{h} \Delta V_M + \Delta I_u^{\text{th}}, \\ \Delta I_r &= (\nu - \nu_i) \frac{e^2}{h} \Delta V_N + \Delta I_r^{\text{th}}, \\ \Delta I_d &= \nu_i \frac{e^2}{h} \Delta V_N + \Delta I_d^{\text{th}},\end{aligned}\tag{S2}$$

where e is the electron charge and h is the Planck's constant. The voltage fluctuations are

$$\begin{aligned}\nu \frac{e^2}{h} \Delta V_M &= \Delta I_S - \Delta I_l^{\text{th}} - \Delta I_u^{\text{th}}, \\ \nu \frac{e^2}{h} \Delta V_N &= \Delta I_G - \Delta I_r^{\text{th}} - \Delta I_d^{\text{th}}.\end{aligned}\tag{S3}$$

From Eq. (S1) we find

$$\begin{aligned}(I_1 - \langle I_1 \rangle) &= \nu_i \frac{e^2}{h} \Delta V_M + \Delta I_u^{\text{th}} + (\nu - \nu_i) \frac{e^2}{h} \Delta V_N + \Delta I_r^{\text{th}} \\ &= \frac{\nu_i}{\nu} \Delta I_S + \frac{(\nu - \nu_i)}{\nu} \Delta I_G \\ &\quad + \frac{(\nu - \nu_i)}{\nu} (\Delta I_u^{\text{th}} - \Delta I_d^{\text{th}}) + \frac{\nu_i}{\nu} (\Delta I_r^{\text{th}} - \Delta I_l^{\text{th}}),\end{aligned}\tag{S4}$$

and

$$\begin{aligned}(I_2 - \langle I_2 \rangle) &= \frac{\nu_i}{\nu} \Delta I_G + \frac{(\nu - \nu_i)}{\nu} \Delta I_S \\ &\quad + \frac{(\nu - \nu_i)}{\nu} (\Delta I_d^{\text{th}} - \Delta I_u^{\text{th}}) + \frac{\nu_i}{\nu} (\Delta I_l^{\text{th}} - \Delta I_r^{\text{th}}).\end{aligned}\tag{S5}$$

We obtain the expressions of $\delta^2 I_1, \delta^2 I_2$ and $\delta^2 I_c$ as

$$\begin{aligned}\delta^2 I_1 &= 2 \left(\frac{e^2}{h} \right) \frac{\nu_i}{\nu} (\nu - \nu_i) k_B (T_M + T_N) \\ &\quad + \frac{1}{\nu^2} \left[\nu_i^2 \langle (\Delta I_S)^2 \rangle + (\nu - \nu_i)^2 \langle (\Delta I_G)^2 \rangle \right],\end{aligned}\tag{S6}$$

$$\begin{aligned}\delta^2 I_2 &= 2 \left(\frac{e^2}{h} \right) \frac{\nu_i}{\nu} (\nu - \nu_i) k_B (T_M + T_N) \\ &\quad + \frac{1}{\nu^2} \left[\nu_i^2 \langle (\Delta I_G)^2 \rangle + (\nu - \nu_i)^2 \langle (\Delta I_S)^2 \rangle \right],\end{aligned}\tag{S7}$$

and

$$\begin{aligned}\delta^2 I_c &= -2 \left(\frac{e^2}{h} \right) \frac{\nu_i}{\nu} (\nu - \nu_i) k_B (T_M + T_N) \\ &\quad + \frac{\nu_i (\nu - \nu_i)}{\nu^2} \left[\langle (\Delta I_G)^2 \rangle + \langle (\Delta I_S)^2 \rangle \right],\end{aligned}\tag{S8}$$

where T_M, T_N are, respectively, the temperatures at the noise spots M and N . To derive Eqs. (S6) to (S8)

we have used the local Johnson-Nyquist relations for thermal noise,

$$\begin{aligned}\langle (\Delta I_l^{\text{th}})^2 \rangle &= \frac{2e^2}{h} (\nu - \nu_i) k_B T_M, \\ \langle (\Delta I_u^{\text{th}})^2 \rangle &= \frac{2e^2}{h} \nu_i k_B T_M, \\ \langle (\Delta I_r^{\text{th}})^2 \rangle &= \frac{2e^2}{h} (\nu - \nu_i) k_B T_N, \\ \langle (\Delta I_d^{\text{th}})^2 \rangle &= \frac{2e^2}{h} \nu_i k_B T_N, \\ \langle (\Delta I_i^{\text{th}} \Delta I_j^{\text{th}}) \rangle &= 0, \text{ for } i \neq j \text{ and } i, j \in \{l, u, r, d\},\end{aligned}\tag{S9}$$

where k_B is the Boltzmann constant. The Fano factors are then defined as

$$F_j = \frac{|\delta^2 I_j|}{2e \langle I \rangle t (1-t)},\tag{S10}$$

where $j \in \{1, 2, c\}$, I is the source current and $t = \langle I_1 \rangle / \langle I \rangle$.

SIII. EXPRESSION FOR THE CCC FOR THREE SPECIFIC CASES OF EDGE EQUILIBRATIONS

We assume that the charge is fully equilibrated, hence charge transport is ballistic, moving ‘‘downstream’’ along each segment of the device (Fig. S1). We call the direction opposite to charge flow (‘‘upstream’’) antiballistic. For the cases we consider, heat is also equilibrated and heat transport can be either ballistic or antiballistic in each segment of the device. Specifically we calculate CCC for the following three cases:

- 1) heat transport is ballistic in ‘‘outer’’, antiballistic in ‘‘line’’, and ballistic in ‘‘upper’’ segments,
- 2) heat transport is antiballistic in ‘‘outer’’, antiballistic in ‘‘line’’, and ballistic in ‘‘upper’’ segments,
- 3) heat transport is ballistic in ‘‘outer’’, ballistic in ‘‘line’’, and antiballistic in ‘‘upper’’ segments.

A. CCC when heat transport is ballistic in ‘‘outer’’, antiballistic in ‘‘line’’, and ballistic in ‘‘upper’’ segments

We consult Fig. S3 and derive expressions of CCC when heat transport is ballistic in ‘‘outer’’, antiballistic in ‘‘line’’, and ballistic in ‘‘upper’’ segments.

1. Temperature calculation

We refer to Fig. S3. Here we calculate the expression of the temperatures T_M, T_N at the noise spots M, N , respectively. We assume zero temperature in the con-

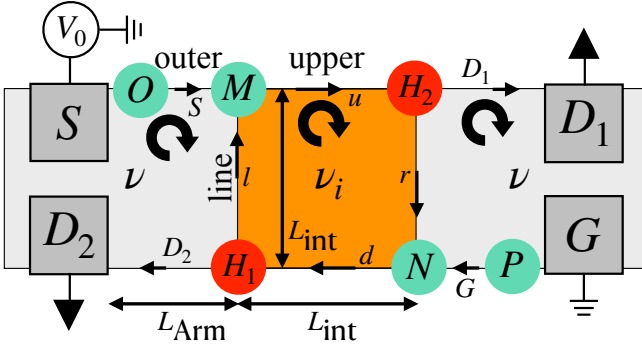


FIG. S3. Noise generation in our proposed device (see Fig. S1): Charge is fully equilibrated, hence charge transport is ballistic, moving “downstream” along each segment of the device. Each circular arrow shows the chirality of charge propagation of the respective filling. We call the direction opposite to charge flow (“upstream”) antiballistic. Heat is also equilibrated and the heat transport is ballistic in “outer”, antiballistic in “line”, and ballistic in “upper” segments, as shown by the arrows. Voltage drops occur at the hot spots H_1, H_2 (red circles), resulting in the noise spots M, N, O, P (green circles) [1].

tacts/leads. Conservation of energy at H_1, N, H_2, M implies the following expressions [1]:

$$\begin{aligned} J_{D_2} + J_l &= P_{H_1} + J_d, \\ J_G + J_r &= J_d, \\ J_{D_1} + J_r &= P_{H_2} + J_u, \\ J_S + J_l &= J_u, \end{aligned} \quad (\text{S11})$$

where J_i is the heat current along $i \in \{S, G, D_1, D_2, u, r, d, l\}$ th segment, and P_{H_1}, P_{H_2} are, respectively, the dissipated powers in the hot spots H_1, H_2 . We write

$$\begin{aligned} J_S &= 0, \quad J_u = \frac{\kappa}{2} T_M^2 (\delta c)_u, \quad J_{D_1} = \frac{\kappa}{2} T_{H_2}^2 (\delta c)_1, \\ J_G &= 0, \quad J_d = \frac{\kappa}{2} T_N^2 (\delta c)_d, \quad J_{D_2} = \frac{\kappa}{2} T_{H_1}^2 (\delta c)_2, \\ J_l &= \frac{\kappa}{2} T_{H_1}^2 (\delta c)_l, \quad J_r = \frac{\kappa}{2} T_{H_2}^2 (\delta c)_r, \end{aligned} \quad (\text{S12})$$

where

$$\kappa = \frac{\pi^2 k_B^2}{3h}, \quad P_{H_1} = P_{H_2} = \frac{e^2 V_0^2 (\nu - \nu_i) \nu_i}{h 2\nu}, \quad (\text{S13})$$

and $T_M, T_N, T_{H_1}, T_{H_2}$ are the temperatures at M, N, H_1, H_2 respectively. The dissipated powers P_{H_1}, P_{H_2} arise due to the Joule heating of the associated voltage drop at H_1, H_2 , respectively. We obtain $P_{H_1} = P_{H_2}$, since the voltage drop only depends on ν and ν_i [1]. Here $(\delta c)_i = |c_{\text{down}} - c_{\text{up}}|_i$ is the modulus of difference between the central charges of downstream and upstream modes in the i th segment of the device.

Taking all these into account we find

$$\begin{aligned} \frac{\kappa}{2} T_{H_1}^2 (\delta c)_2 + \frac{\kappa}{2} T_{H_1}^2 (\delta c)_l &= P_{H_1} + \frac{\kappa}{2} T_N^2 (\delta c)_d, \\ 0 + \frac{\kappa}{2} T_{H_2}^2 (\delta c)_r &= \frac{\kappa}{2} T_N^2 (\delta c)_d, \\ \frac{\kappa}{2} T_{H_2}^2 (\delta c)_1 + \frac{\kappa}{2} T_{H_2}^2 (\delta c)_r &= P_{H_2} + \frac{\kappa}{2} T_M^2 (\delta c)_u, \\ 0 + \frac{\kappa}{2} T_{H_1}^2 (\delta c)_l &= \frac{\kappa}{2} T_M^2 (\delta c)_u, \end{aligned} \quad (\text{S14})$$

and hence,

$$\begin{aligned} \frac{[(\delta c)_1 + (\delta c)_r]}{(\delta c)_r} (\delta c)_d \frac{\kappa}{2} T_N^2 &= P_{H_2} + \frac{\kappa}{2} (\delta c)_u T_M^2, \\ \frac{[(\delta c)_2 + (\delta c)_l]}{(\delta c)_l} (\delta c)_u \frac{\kappa}{2} T_M^2 &= P_{H_1} + \frac{\kappa}{2} (\delta c)_d T_N^2. \end{aligned} \quad (\text{S15})$$

Therefore,

$$\begin{aligned} \frac{\kappa}{2} (\delta c)_u T_M^2 \left[1 + \frac{(\delta c)_2 + (\delta c)_l}{(\delta c)_l} \right] & \\ = \frac{\kappa}{2} (\delta c)_d T_N^2 \left[1 + \frac{(\delta c)_1 + (\delta c)_r}{(\delta c)_r} \right]. & \end{aligned} \quad (\text{S16})$$

We note that $(\delta c)_u = (\delta c)_d$, $(\delta c)_2 = (\delta c)_1$, $(\delta c)_l = (\delta c)_r$, hence $T_M = T_N$. Thus we find

$$\frac{\kappa T_M^2 (\delta c)_1}{2 (\delta c)_r} (\delta c)_d = P_{H_2} = \frac{e^2 V_0^2 (\nu - \nu_i) \nu_i}{h 2\nu}, \quad (\text{S17})$$

and, finally,

$$T_M = T_N = \frac{e V_0}{\pi k_B} \sqrt{\frac{3(\nu - \nu_i) \nu_i}{\nu} \frac{(\delta c)_r}{(\delta c)_1 (\delta c)_d}}. \quad (\text{S18})$$

2. Noise spot contributions

We refer to Fig. S3. Here we calculate the contributions $\langle (\Delta I_S)^2 \rangle$, $\langle (\Delta I_G)^2 \rangle$ of the noise spots O, P , respectively. To evaluate $\langle (\Delta I_S)^2 \rangle$, $\langle (\Delta I_G)^2 \rangle$ we need to compute the following integral [1],

$$\begin{aligned} \langle (\Delta I_S)^2 \rangle &= \langle (\Delta I_G)^2 \rangle \\ &= \frac{2e^2}{h l_{\text{eq}}^{\text{ch}}} \nu \frac{\nu_-}{\nu_+} \int_0^{L_{\text{Arm}}} dx \frac{e^{-\frac{2x}{l_{\text{eq}}^{\text{ch}}}} k_B [T_+(x) + T_-(x)]}{\left[1 - \left(e^{-\frac{-L_{\text{Arm}}}{l_{\text{eq}}^{\text{ch}}}} \frac{\nu_-}{\nu_+} \right) \right]^2}, \end{aligned} \quad (\text{S19})$$

where $l_{\text{eq}}^{\text{ch}}$ is the charge equilibration length, $\nu = (\nu_+ - \nu_-)$, and $T_{\pm}(x)$ are the temperature profiles in ν_{\pm} , respectively. We note that $T_{\pm}(x)$ depend on the thermal equilibration length l_{eq} , to be further discussed below. Here ν_+ is the filling factor of the downstream mode and ν_- is the filling factor of the upstream mode.

To compute $T_{\pm}(x)$ we solve the following differential equation for the local temperatures,

$$\begin{bmatrix} \partial_x T_+^2 \\ \partial_x T_-^2 \end{bmatrix} = \frac{\gamma}{l} \begin{bmatrix} -c_{\text{up}} & c_{\text{up}} \\ -c_{\text{down}} & c_{\text{down}} \end{bmatrix} \begin{bmatrix} T_+^2 \\ T_-^2 \end{bmatrix}, \quad (\text{S20})$$

where $l = \frac{(\nu_+ - \nu_-)l_{\text{eq}}}{\nu_+ \nu_-}$ and c_{down} (c_{up}) is the central charge of the downstream (upstream) mode. Here γ is a parameter of order unity, characterizing the deviation of the ratio of intermode charge and heat tunneling conductances from Wiedemann-Franz law [1], where the Wiedemann-Franz law corresponds to $\gamma = 1$. We assume that there are no voltage drops along the ‘‘outer’’ segment (Fig. S3), hence there is no Joule heating contribution in the following [1]. The boundary conditions are

$$T_+(0) = 0, \quad T_-(L_{\text{Arm}}) = T_M. \quad (\text{S21})$$

The temperature profiles are found to be

$$T_+^2 = T_M^2 \left(\frac{c_{\text{up}} - c_{\text{up}} e^{-\alpha x/l_{\text{eq}}}}{c_{\text{up}} - c_{\text{down}} e^{-\alpha L_{\text{Arm}}/l_{\text{eq}}}} \right), \quad (\text{S22})$$

$$T_-^2 = T_M^2 \left(\frac{c_{\text{up}} - c_{\text{down}} e^{-\alpha x/l_{\text{eq}}}}{c_{\text{up}} - c_{\text{down}} e^{-\alpha L_{\text{Arm}}/l_{\text{eq}}}} \right),$$

where $\alpha = \frac{-(c_{\text{down}} - c_{\text{up}})\gamma\nu_+\nu_-}{\nu}$. Plugging the temperature profiles into Eq. (S19), we can derive the expression of $\langle(\Delta I_S)^2\rangle = \langle(\Delta I_G)^2\rangle$. We note that for full thermal equilibration with length $l_{\text{eq}}^{\text{full}}$, we have $l_{\text{eq}} = l_{\text{eq}}^{\text{full}}$, while for partial thermal equilibration with length $l_{\text{eq}}^{\text{par}}$, we have $l_{\text{eq}} = l_{\text{eq}}^{\text{par}}$. We are interested in the limit where $L_{\text{Arm}} \gg l_{\text{eq}}$ and $L_{\text{Arm}} \gg l_{\text{eq}}^{\text{ch}}$.

B. CCC when heat transport is antiballistic in ‘‘outer’’, antiballistic in ‘‘line’’, and ballistic in ‘‘upper’’ segments

We consult Fig. S4 and derive expressions for the CCC when heat transport is antiballistic in ‘‘outer’’, antiballistic in ‘‘line’’, and ballistic in ‘‘upper’’ segments.

1. Temperature calculation

We refer to Fig. S4. Here we calculate the expression for the temperatures T_M, T_N at the noise spots M, N , respectively. We assume zero temperature in the contacts/leads. Conservation of energy at H_1, N, H_2, M implies the following expressions [1]:

$$\begin{aligned} J_l &= J_{D_2} + P_{H_1} + J_d, \\ J_G + J_d &= J_r, \\ J_r &= J_{D_1} + P_{H_2} + J_u, \\ J_S + J_u &= J_l, \end{aligned} \quad (\text{S23})$$

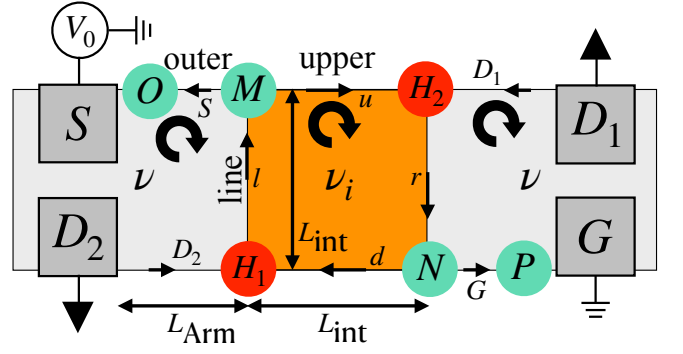


FIG. S4. Noise generation in our proposed device (see Fig. S1): Charge is fully equilibrated, hence charge transport is ballistic, moving ‘‘downstream’’ along each segment of the device. Each circular arrow shows the chirality of charge propagation of the respective filling. We call the direction opposite to charge flow (‘‘upstream’’) antiballistic. Heat is also equilibrated and the heat transport is antiballistic in ‘‘outer’’, antiballistic in ‘‘line’’, and ballistic in ‘‘upper’’ segments, as shown by the arrows. Voltage drops occur at the hot spots H_1, H_2 (red circles), resulting in noise spots M, N, O, P (green circles) [1].

where J_i is the heat current along $i \in \{S, G, D_1, D_2, u, r, d, l\}$ th segment, and P_{H_1}, P_{H_2} are, respectively, the dissipated powers in the hot spots H_1, H_2 . We write

$$\begin{aligned} J_S &= \frac{\kappa}{2} T_M^2 (\delta c)_S, \quad J_u = \frac{\kappa}{2} T_M^2 (\delta c)_u, \quad J_{D_1} = 0, \\ J_G &= \frac{\kappa}{2} T_N^2 (\delta c)_G, \quad J_d = \frac{\kappa}{2} T_N^2 (\delta c)_d, \quad J_{D_2} = 0, \\ J_l &= \frac{\kappa}{2} T_{H_1}^2 (\delta c)_l, \quad J_r = \frac{\kappa}{2} T_{H_2}^2 (\delta c)_r, \end{aligned} \quad (\text{S24})$$

where

$$\kappa = \frac{\pi^2 k_B^2}{3h}, \quad P_{H_1} = P_{H_2} = \frac{e^2 V_0^2 (\nu - \nu_i) \nu_i}{h 2\nu}, \quad (\text{S25})$$

and $T_M, T_N, T_{H_1}, T_{H_2}$ are the temperatures at M, N, H_1, H_2 , respectively. The dissipated powers P_{H_1}, P_{H_2} arise due to the Joule heating of the associated voltage drop at H_1, H_2 , respectively. We obtain $P_{H_1} = P_{H_2}$, since the voltage drop only depends on ν and ν_i [1]. Here $(\delta c)_i = |(c_{\text{down}} - c_{\text{up}})_i|$ is the modulus of difference between the central charges of downstream and upstream modes in the i th segment of the device.

With all these in mind we find

$$\begin{aligned} \frac{\kappa}{2} T_{H_1}^2 (\delta c)_l &= 0 + P_{H_1} + \frac{\kappa}{2} T_N^2 (\delta c)_d, \\ \frac{\kappa}{2} T_N^2 (\delta c)_G + \frac{\kappa}{2} T_N^2 (\delta c)_d &= \frac{\kappa}{2} T_{H_2}^2 (\delta c)_r, \\ \frac{\kappa}{2} T_{H_2}^2 (\delta c)_r &= 0 + P_{H_2} + \frac{\kappa}{2} T_M^2 (\delta c)_u, \\ \frac{\kappa}{2} T_M^2 (\delta c)_S + \frac{\kappa}{2} T_M^2 (\delta c)_u &= \frac{\kappa}{2} T_{H_1}^2 (\delta c)_l, \end{aligned} \quad (\text{S26})$$

and thus

$$\begin{aligned} [(\delta c)_G + (\delta c)_d] \frac{\kappa}{2} T_N^2 &= P_{H_2} + \frac{\kappa}{2} (\delta c)_u T_M^2, \\ [(\delta c)_S + (\delta c)_u] \frac{\kappa}{2} T_M^2 &= P_{H_1} + \frac{\kappa}{2} (\delta c)_d T_N^2. \end{aligned} \quad (\text{S27})$$

Therefore,

$$T_M^2 = \frac{[(\delta c)_G + 2(\delta c)_d]}{[(\delta c)_S + 2(\delta c)_u]} T_N^2. \quad (\text{S28})$$

We note that $(\delta c)_u = (\delta c)_d$, $(\delta c)_2 = (\delta c)_1$, $(\delta c)_l = (\delta c)_r$, $(\delta c)_S = (\delta c)_G$, hence $T_M = T_N$. Thus we find

$$T_M = T_N = \frac{eV_0}{\pi k_B} \sqrt{\frac{3(\nu - \nu_i)\nu_i}{\nu} \frac{1}{(\delta c)_G}}. \quad (\text{S29})$$

2. Noise spot contributions

To calculate the contributions $\langle(\Delta I_S)^2\rangle$, $\langle(\Delta I_G)^2\rangle$ from the noise spots O, P , respectively, we can use the same equations as in Section SII A 2.

C. CCC when heat transport is ballistic in “outer”, ballistic in “line”, and antiballistic in “upper” segments

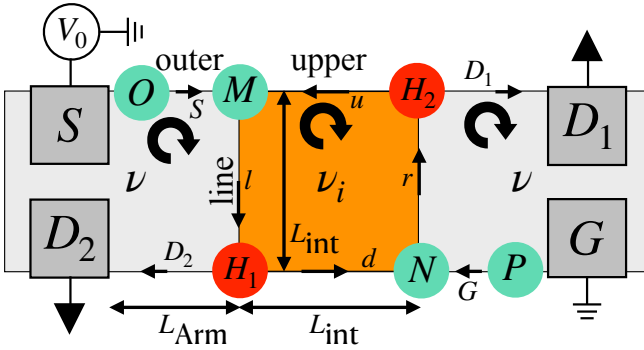


FIG. S5. Noise generation in our proposed device (see Fig. S1): Charge is fully equilibrated, hence charge transport is ballistic, moving “downstream” along each segment of the device. Each circular arrow shows the chirality of charge propagation of the respective filling. We call the direction opposite to charge flow (“upstream”) antiballistic. Heat is also equilibrated and the heat transport is ballistic in “outer”, ballistic in “line”, and antiballistic in “upper” segments, as shown by the arrows. Voltage drops occur at the hot spots H_1, H_2 (red circles), resulting in noise spots M, N, O, P (green circles) [1].

We consult Fig. S5 and derive expressions for the CCC when heat transport is ballistic in “outer”, ballistic in “line”, and antiballistic in “upper” segments.

1. Temperature calculation

We refer to Fig. S5. Here we calculate the expression of the temperatures T_M, T_N at the noise spots M, N , respectively. We assume zero temperature in the contacts/leads. Conservation of energy at H_1, N, H_2, M implies the following expressions [1]:

$$\begin{aligned} J_{D_2} + J_d &= P_{H_1} + J_l, \\ J_G + J_d &= J_r, \\ J_{D_1} + J_u &= P_{H_2} + J_r, \\ J_S + J_u &= J_l, \end{aligned} \quad (\text{S30})$$

where J_i is the heat current along $i \in \{S, G, D_1, D_2, u, r, d, l\}$ th segment, and P_{H_1}, P_{H_2} are, respectively, the dissipated powers in the hot spots H_1, H_2 . We write

$$\begin{aligned} J_S &= 0, \quad J_u = \frac{\kappa}{2} T_{H_2}^2 (\delta c)_u, \quad J_{D_1} = \frac{\kappa}{2} T_{H_2}^2 (\delta c)_1, \\ J_G &= 0, \quad J_d = \frac{\kappa}{2} T_{H_1}^2 (\delta c)_d, \quad J_{D_2} = \frac{\kappa}{2} T_{H_1}^2 (\delta c)_2, \\ J_l &= \frac{\kappa}{2} T_M^2 (\delta c)_l, \quad J_r = \frac{\kappa}{2} T_N^2 (\delta c)_r, \end{aligned} \quad (\text{S31})$$

where

$$\kappa = \frac{\pi^2 k_B^2}{3h}, \quad P_{H_1} = P_{H_2} = \frac{e^2 V_0^2 (\nu - \nu_i) \nu_i}{h 2\nu}, \quad (\text{S32})$$

and $T_M, T_N, T_{H_1}, T_{H_2}$ are the temperatures at M, N, H_1, H_2 , respectively. The dissipated powers P_{H_1}, P_{H_2} arise due to the Joule heating of the associated voltage drop at H_1, H_2 , respectively. We obtain $P_{H_1} = P_{H_2}$, since the voltage drop only depends on ν and ν_i [1]. Here $(\delta c)_i = |(c_{\text{down}} - c_{\text{up}})_i|$ is the modulus of difference between the central charges of downstream and upstream modes in the i th segment of the device.

Thereby we find

$$\begin{aligned} \frac{\kappa}{2} T_{H_1}^2 (\delta c)_2 + \frac{\kappa}{2} T_{H_1}^2 (\delta c)_d &= P_{H_1} + \frac{\kappa}{2} T_M^2 (\delta c)_l, \\ 0 + \frac{\kappa}{2} T_{H_1}^2 (\delta c)_d &= \frac{\kappa}{2} T_N^2 (\delta c)_r, \\ \frac{\kappa}{2} T_{H_2}^2 (\delta c)_1 + \frac{\kappa}{2} T_{H_2}^2 (\delta c)_u &= P_{H_2} + \frac{\kappa}{2} T_N^2 (\delta c)_r, \\ 0 + \frac{\kappa}{2} T_{H_2}^2 (\delta c)_u &= \frac{\kappa}{2} T_M^2 (\delta c)_l, \end{aligned} \quad (\text{S33})$$

and hence,

$$\begin{aligned} [(\delta c)_2 + (\delta c)_d] \frac{\kappa}{2} T_{H_1}^2 &= P_{H_1} + \frac{\kappa}{2} (\delta c)_l T_M^2, \\ [(\delta c)_1 + (\delta c)_u] \frac{\kappa}{2} T_{H_2}^2 &= P_{H_2} + \frac{\kappa}{2} (\delta c)_r T_N^2. \end{aligned} \quad (\text{S34})$$

Therefore,

$$\begin{aligned} T_N^2 \left[\frac{(\delta c)_r}{(\delta c)_d} ((\delta c)_2 + (\delta c)_d) + (\delta c)_r \right] \\ = T_M^2 \left[\frac{(\delta c)_l}{(\delta c)_u} ((\delta c)_1 + (\delta c)_u) + (\delta c)_l \right]. \end{aligned} \quad (\text{S35})$$

We note that $(\delta c)_u = (\delta c)_d$, $(\delta c)_2 = (\delta c)_1$, $(\delta c)_l = (\delta c)_r$, $(\delta c)_S = (\delta c)_G$, hence $T_M = T_N$. Thus we find

$$T_M = T_N = \frac{eV_0}{\pi k_B} \sqrt{\frac{3(\nu - \nu_i)\nu_i}{\nu}} \left[\frac{(\delta c)_r}{(\delta c)_d} ((\delta c)_2 + (\delta c)_d) - (\delta c)_l \right]^{-\frac{1}{2}}. \quad (\text{S36})$$

2. Noise spot contributions

To calculate the contributions $\langle(\Delta I_S)^2\rangle$, $\langle(\Delta I_G)^2\rangle$ from the noise spots O, P , respectively, we can use the same equations as in Section SII A 2.

SIII. COMPUTATION OF CCC VALUES

Here we compute the CCC for specific choices of $\{\nu, \nu_i\}$ and for the Pf, APf, and PHPf states and different edge equilibration regimes.

A. $\{\nu, \nu_i\} = \{5/2, 2\}$ with an APf state and full thermal equilibration

Here heat transport is ballistic in “outer”, antiballistic in “line”, and ballistic in “upper” segments, and we consult Section SII A and Fig. S3. From Eq. (S18) with $\{\nu, \nu_i\} = \{5/2, 2\}$, $(\delta c)_r = 1/2$, $(\delta c)_1 = 3/2$, and $(\delta c)_d = 2$ we find

$$T_M = T_N = \frac{eV_0}{\sqrt{5}\pi k_B}. \quad (\text{S37})$$

Here we have $l_{\text{eq}} = l_{\text{eq}}^{\text{full}}$. We note that the “outer” segment is in the ballistic regime. Hence, we expect an exponential suppression of $\langle(\Delta I_S)^2\rangle = \langle(\Delta I_G)^2\rangle$ [1]. Therefore, we find

$$\delta^2 I_1 = \delta^2 I_2 = |\delta^2 I_c| = \frac{8e^3 V_0}{5\sqrt{5}\pi h} \approx 0.227 \frac{e^3 V_0}{h}. \quad (\text{S38})$$

The source current is $I = 5e^2 V_0 / (2h)$, while the transmission coefficient is $t = 2 / (5/2) = 4/5$. We thus obtain the corresponding Fano factors,

$$F_1 = F_2 = |F_c| = \frac{\delta^2 I_1}{2eIt(1-t)} = \frac{2}{\sqrt{5}\pi} \approx 0.284. \quad (\text{S39})$$

B. $\{\nu, \nu_i\} = \{5/2, 7/3\}$ with a PHPf state and full thermal equilibration

Here heat transport is ballistic in “outer”, antiballistic in “line”, and ballistic in “upper” segments, and we consult Section SII A and Fig. S3. From Eq. (S18) with

$\{\nu, \nu_i\} = \{5/2, 7/3\}$, $(\delta c)_r = 1/2$, $(\delta c)_1 = 5/2$, and $(\delta c)_d = 3$ we find

$$T_M = T_N = \frac{\sqrt{7}eV_0}{15\pi k_B}. \quad (\text{S40})$$

Here we have $l_{\text{eq}} = l_{\text{eq}}^{\text{full}}$. We note that the “outer” segment is in the ballistic regime. Hence, we expect an exponential suppression of $\langle(\Delta I_S)^2\rangle = \langle(\Delta I_G)^2\rangle$ [1]. Therefore, we find

$$\delta^2 I_1 = \delta^2 I_2 = |\delta^2 I_c| = \frac{28\sqrt{7}e^3 V_0}{675\pi h} \approx 0.0349 \frac{e^3 V_0}{h}. \quad (\text{S41})$$

The source current is $I = 5e^2 V_0 / (2h)$, while the transmission coefficient is $t = (7/3) / (5/2) = 14/15$. We thus obtain the corresponding Fano factors,

$$F_1 = F_2 = |F_c| = \frac{\delta^2 I_1}{2eIt(1-t)} \approx 0.112. \quad (\text{S42})$$

C. $\{\nu, \nu_i\} = \{5/2, 7/3\}$ with an APf state and full thermal equilibration

Here heat transport is ballistic in “outer”, antiballistic in “line”, and ballistic in “upper” segments, and we consult Section SII A and Fig. S3. From Eq. (S18) with $\{\nu, \nu_i\} = \{5/2, 7/3\}$, $(\delta c)_r = 3/2$, $(\delta c)_1 = 3/2$, and $(\delta c)_d = 3$ we find

$$T_M = T_N = \frac{\sqrt{7}eV_0}{\sqrt{45}\pi k_B}. \quad (\text{S43})$$

Here we have $l_{\text{eq}} = l_{\text{eq}}^{\text{full}}$. We note that the “outer” segment is in the ballistic regime. Hence, we expect an exponential suppression of $\langle(\Delta I_S)^2\rangle = \langle(\Delta I_G)^2\rangle$ [1]. Therefore, we find

$$\delta^2 I_1 = \delta^2 I_2 = |\delta^2 I_c| = \frac{28\sqrt{7}e^3 V_0}{45\sqrt{45}\pi h} \approx 0.078 \frac{e^3 V_0}{h}. \quad (\text{S44})$$

The source current is $I = 5e^2 V_0 / (2h)$, while the transmission coefficient is $t = (7/3) / (5/2) = 14/15$. We thus obtain the corresponding Fano factors,

$$F_1 = F_2 = |F_c| = \frac{\delta^2 I_1}{2eIt(1-t)} \approx 0.2507. \quad (\text{S45})$$

D. $\{\nu, \nu_i\} = \{5/2, 7/3\}$ with a PHPf state and partial thermal equilibration

Here heat transport is ballistic in “outer”, antiballistic in “line”, and ballistic in “upper” segments, and we consult Section SII A and Fig. S3. We note that for partial thermal equilibration, the counter-propagating modes in the lowest Landau levels of ν and ν_i localize in the “line” segment and do not contribute to the CCC, while the

modes in the second Landau levels do contribute. We effectively have the fillings $\{\nu^{\text{eff}}, \nu_i^{\text{eff}}\} = \{1/2, 1/3\}$ for $\{\nu, \nu_i\} = \{5/2, 7/3\}$. From Eq. (S18) with $\{\nu^{\text{eff}}, \nu_i^{\text{eff}}\} = \{1/2, 1/3\}$, $(\delta c)_r = 1/2$, $(\delta c)_1 = 1/2$, and $(\delta c)_d = 1$ we find

$$T_M = T_N = \frac{eV_0}{\sqrt{3}\pi k_B}. \quad (\text{S46})$$

Here we have $l_{\text{eq}} = l_{\text{eq}}^{\text{par}}$. We note that the “outer” segment is in the ballistic regime. Hence, we expect an exponential suppression of $\langle(\Delta I_S)^2\rangle = \langle(\Delta I_G)^2\rangle$ [1]. Therefore, we find

$$\delta^2 I_1 = \delta^2 I_2 = |\delta^2 I_c| = \frac{4e^3 V_0}{9\sqrt{3}\pi h} \approx 0.0816 \frac{e^3 V_0}{h}. \quad (\text{S47})$$

The source current is $I = 5e^2 V_0/(2h)$, while the transmission coefficient is $t = (7/3)/(5/2) = 14/15$. We thus obtain the corresponding Fano factors,

$$F_1 = F_2 = |F_c| = \frac{\delta^2 I_1}{2eIt(1-t)} \approx 0.2625. \quad (\text{S48})$$

E. $\{\nu, \nu_i\} = \{5/2, 7/3\}$ with an APf state and partial thermal equilibration

Here heat transport is antiballistic in “outer”, antiballistic in “line”, and ballistic in “upper” segments, and we consult Section SII B and Fig. S4. We note that for partial thermal equilibration, the counter-propagating modes in the lowest Landau levels of ν and ν_i localize in the “line” segment and do not contribute to the CCC, while the modes in the second Landau levels do contribute. We effectively have the filling $\{\nu^{\text{eff}}, \nu_i^{\text{eff}}\} = \{1/2, 1/3\}$ for $\{\nu, \nu_i\} = \{5/2, 7/3\}$. From Eq. (S29) with $\{\nu^{\text{eff}}, \nu_i^{\text{eff}}\} = \{1/2, 1/3\}$, $(\delta c)_G = 1/2$ we find

$$T_M = T_N = \frac{\sqrt{2}}{\sqrt{3}} \frac{eV_0}{\pi k_B}. \quad (\text{S49})$$

Here we have $l_{\text{eq}} = l_{\text{eq}}^{\text{par}}$. We note that the “outer” segment is in the antiballistic regime. Therefore, a constant noise for $\langle(\Delta I_S)^2\rangle = \langle(\Delta I_G)^2\rangle$ is expected [1]. We use Ref. 1 to calculate $\langle(\Delta I_S)^2\rangle = \langle(\Delta I_G)^2\rangle$,

$$\begin{aligned} \langle(\Delta I_S)^2\rangle = \langle(\Delta I_G)^2\rangle &= \frac{e^2}{h} \nu^{\text{eff}} \left(\frac{\nu_-}{\nu_+} \right) k_B T_M \\ &\times \left[\frac{\sqrt{\pi} \Gamma(\frac{2+\alpha}{\alpha})}{2\Gamma(\frac{3}{2} + \frac{\alpha}{2})} + {}_2F_1 \left(-\frac{1}{2}, \frac{2}{\alpha}; \frac{2+\alpha}{\alpha}; \frac{c_{\text{down}}}{c_{\text{up}}} \right) \right], \end{aligned} \quad (\text{S50})$$

where $\nu^{\text{eff}} = 1/2$, $\nu_+ = 1$, $\nu_- = 1/2$, $k_B T_M = \sqrt{2}eV_0/(\sqrt{3}\pi)$, $\gamma = 1$, $c_{\text{down}} = 1$, $c_{\text{up}} = 3/2$, $\alpha = -(c_{\text{down}} - c_{\text{up}})\gamma\nu_+\nu_-/\nu^{\text{eff}} = 1/2$. We find $\langle(\Delta I_S)^2\rangle = \langle(\Delta I_G)^2\rangle \approx 0.07e^3 V_0/h$. Therefore, we obtain

$$(\delta^2 I_1 = \delta^2 I_2) \approx 0.1543 \frac{e^3 V_0}{h}, \quad \delta^2 I_c \approx -0.0845 \frac{e^3 V_0}{h}. \quad (\text{S51})$$

The source current is $I = 5e^2 V_0/(2h)$, while the transmission coefficient is $t = (7/3)/(5/2) = 14/15$. We thus obtain the corresponding Fano factors,

$$F_1 = F_2 = \frac{\delta^2 I_1}{2eIt(1-t)} \approx 0.4959, \quad |F_c| \approx 0.271. \quad (\text{S52})$$

F. $\{\nu, \nu_i\} = \{3, 5/2\}$ with a Pf state and full thermal equilibration

Here heat transport is ballistic in “outer”, antiballistic in “line”, and ballistic in “upper” segments, and we consult Section SII A and Fig. S3. From Eq. (S18) with $\{\nu, \nu_i\} = \{3, 5/2\}$, $(\delta c)_r = 1/2$, $(\delta c)_1 = 3$, and $(\delta c)_d = 7/2$ we find

$$T_M = T_N \approx 0.077 \frac{eV_0}{k_B}. \quad (\text{S53})$$

Here we have $l_{\text{eq}} = l_{\text{eq}}^{\text{full}}$. We note that the “outer” segment is in the ballistic regime. Hence, we expect an exponential suppression of $\langle(\Delta I_S)^2\rangle = \langle(\Delta I_G)^2\rangle$ [1]. Therefore, we find

$$\delta^2 I_1 = \delta^2 I_2 = |\delta^2 I_c| \approx 0.128 \frac{e^3 V_0}{h}. \quad (\text{S54})$$

The source current is $I = 3e^2 V_0/h$, while the transmission coefficient is $t = (5/2)/3 = 5/6$. We thus obtain the corresponding Fano factors,

$$F_1 = F_2 = |F_c| = \frac{\delta^2 I_1}{2eIt(1-t)} \approx 0.155. \quad (\text{S55})$$

G. $\{\nu, \nu_i\} = \{3, 5/2\}$ with a Pf state and partial thermal equilibration

Here heat transport is ballistic in “outer”, antiballistic in “line”, and ballistic in “upper” segments, and we consult Section SII A and Fig. S3. We note that for partial thermal equilibration, the counter-propagating modes in the lowest Landau levels of ν and ν_i localize in the “line” segment and do not contribute to the CCC, while the modes in the second Landau levels do contribute. We effectively have the filling $\{\nu^{\text{eff}}, \nu_i^{\text{eff}}\} = \{1, 1/2\}$ for $\{\nu, \nu_i\} = \{3, 5/2\}$. From Eq. (S18) with $\{\nu^{\text{eff}}, \nu_i^{\text{eff}}\} = \{1, 1/2\}$, $(\delta c)_r = 1/2$, $(\delta c)_1 = 1$, and $(\delta c)_d = 3/2$ we find

$$T_M = T_N = 0.5 \frac{eV_0}{\pi k_B}. \quad (\text{S56})$$

Here we have $l_{\text{eq}} = l_{\text{eq}}^{\text{par}}$. We note that the “outer” segment is in the ballistic regime. Hence, we expect an exponential suppression of $\langle(\Delta I_S)^2\rangle = \langle(\Delta I_G)^2\rangle$ [1]. Therefore, we find

$$\delta^2 I_1 = \delta^2 I_2 = |\delta^2 I_c| = 0.5 \frac{e^3 V_0}{\pi h}. \quad (\text{S57})$$

The source current is $I = 3e^2V_0/(h)$, while the transmission coefficient is $t = (5/2)/3 = 5/6$. We thus obtain the corresponding Fano factors,

$$F_1 = F_2 = |F_c| = \frac{\delta^2 I_1}{2eIt(1-t)} \approx 0.19. \quad (\text{S58})$$

H. $\{\nu, \nu_i\} = \{3, 5/2\}$ with an APf state and partial thermal equilibration

Here heat transport is ballistic in “outer”, ballistic in “line”, and antiballistic in “upper” segments, and we consult Section SII C and Fig. S5. We note that for partial thermal equilibration, the counter-propagating modes in the lowest Landau levels of ν and ν_i localize in the “line” segment and do not contribute to the CCC, while the modes in the second Landau levels do contribute. We effectively have the filling $\{\nu^{\text{eff}}, \nu_i^{\text{eff}}\} = \{1, 1/2\}$ for $\{\nu, \nu_i\} = \{3, 5/2\}$. From Eq. (S36) with $\{\nu^{\text{eff}}, \nu_i^{\text{eff}}\} =$

$\{1, 1/2\}$, $(\delta c)_r = 3/2$, $(\delta c)_d = 1/2$, $(\delta c)_2 = 1$, and $(\delta c)_l = 3/2$ we find

$$T_M = T_N = 0.5 \frac{eV_0}{\pi k_B}. \quad (\text{S59})$$

Here we have $l_{\text{eq}} = l_{\text{eq}}^{\text{par}}$. We note that the “outer” segment is in the ballistic regime. Hence, we expect an exponential suppression of $\langle(\Delta I_S)^2\rangle = \langle(\Delta I_G)^2\rangle$ [1]. Therefore, we find

$$\delta^2 I_1 = \delta^2 I_2 = |\delta^2 I_c| = 0.5 \frac{e^3 V_0}{\pi h}. \quad (\text{S60})$$

The source current is $I = 3e^2V_0/(h)$, while the transmission coefficient is $t = (5/2)/3 = 5/6$. We thus obtain the corresponding Fano factors,

$$F_1 = F_2 = |F_c| = \frac{\delta^2 I_1}{2eIt(1-t)} = 0.6. \quad (\text{S61})$$

[1] C. Spånslätt, J. Park, Y. Gefen, and A. D. Mirlin, Conductance plateaus and shot noise in fractional quantum hall point contacts, Phys. Rev. B **101**, 075308 (2020).